JOC Article

Theoretical and Experimental Studies on the Baeyer−Villiger Oxidation of Ketones and the Effect of α-Halo Substituents

Friedrich Grein,*,† Austin C. Chen,‡ David Edwards,§ and Cathleen M. Crudden*,§

Department of Chemistry, University of New Brunswick, Fredericton, New Brunswick, E3B 6E2, Canada, and Department of Chemistry, Queen's University, Kingston, Ontario K7L 3N6, Canada

fritz@unb.ca; cruddenc@chem.queensu.ca

Received July 6, 2005

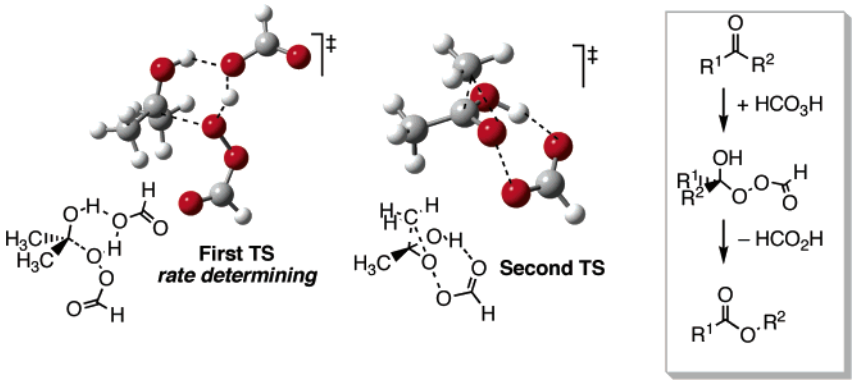

The Baeyer−Villiger reactions of acetone and 3-pentanone, including their fluorinated and chlorinated derivatives, with performic acid have been studied by ab initio and DFT calculations. Results are compared with experimental findings for the Baeyer−Villiger oxidation of aliphatic fluoro and chloroketones. According to theoretical results, the first transition state is rate-determining for all substrates even in the presence of acid catalyst. Although the introduction of acid into the reaction pathway leads to a dramatic decrease in the activation energy for the first transition state (TS), once entropy is included in the calculations, the enthalpic gain is lost. Of all substrates examined, pentanone reacts with performic acid via the lowest energy transition state. The second transition state is also lowest for pentanone, illustrating the accelerating effect of the additional alkyl group. Interestingly, there is only a small energetic difference in the transition states leading to migration of the fluorinated substituent versus the alkyl substituent in fluoropentanone and fluoroacetone. These differences match remarkably well with the experimentally obtained ratios of oxidation at the fluorinated and nonfluorinated carbons in a series of aliphatic ketones (calculated, 0.3 kcal/mol, observed, 0.5 kcal/mol), which are reported herein. The migration of the chlorinated substituent is significantly more difficult than that of the alkyl, with a difference in the second transition state of approximately 2.6 kcal/mol.

1. Introduction

The Baeyer−Villiger reaction,[1] in which a ketone is converted into an ester or lactone upon treatment with a peracid, is a valuable reaction because of the importance of the products, the uniqueness of the transformation, and the difficulty of accomplishing it by other means.[2,3] The basic mechanism of the reaction was described by Criegee more than 50 years ago.[4] First the peracid attacks the carbonyl carbon, leading to a hemiperacetal (also known as the Criegee intermediate), and then one of the adjacent carbon−carbon bonds migrates to the perester oxygen, reforming the carbonyl with loss of a proton and cleavage of the O−O bond (eq 1).

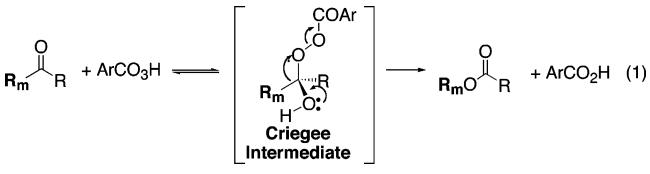

(1)

† University of New Brunswick.
‡ Current address: Merck Frosst Center for Therapeutic Research, Montreal, PQ, Canada.
§ Queen's University.

(1) Baeyer, A.; Villiger, V. *Chem. Ber.* **1899**, *32*, 3625.

10.1021/jo0513966 CCC: $33.50 © 2006 American Chemical Society
Published on Web 01/11/2006

In unsymmetrical ketones, migration of the two substituents leads to different products. The relative ease of migration of a given substituent is called its *migratory aptitude*. It has been empirically determined that substituents that are best able to stabilize a positive charge migrate preferentially and are said to have higher migratory aptitudes.[2] Despite the utility of this rule for predicting regioselectivity, relatively subtle differences in structure can have significant effects on the migratory aptitudes of carbonyl substituents.[5−7] Since being able to predict the position of oxidation is crucial for the application of this reaction to the synthesis of complex organic compounds, understanding migratory aptitudes is critical.

In addition to the uncertainty involved in predicting relative migratory aptitudes, the question of whether the first or second step of the reaction is rate-determining is also under debate. In the 1950s, Hawthorne and Emmons[9] proposed that the reaction occurs by a rate-limiting, acid-catalyzed migration. Simamura and co-workers came to a similar conclusion after their kinetic studies.[10] Palmer and Fry, however,[11] cited the observation of kinetic isotope effects (^{14}C) and a negative ρ value for the Hammett plot of a series of *p*-substituted acetophenone substrates as conclusive evidence for a rate-determining migration. However, others have interpreted the ^{14}C labeling studies as evidence of a switch from rate-determining migration to rate-determining addition to the carbonyl depending on the electron-withdrawing or -donating nature of the ketone substituents.[2,3,12−14] Ogata also interpreted extensive kinetic data for the oxidation of substituted benzaldehydes in terms of a switch in the rate-determining step from migration to addition.[14] Recent computational studies by Reyes et al. support the switch in mechanism from rate-determining migration for electron-withdrawing ketones to rate-determining addition for electron-rich ketones.[12] Intra and intermolecular kinetic isotope effects in the oxidation of cyclohexanone provide strong evidence that the first step is rate-determining in the systems examined in this study.[15]

The effect of acid on the reaction must also be considered.[16,17] Doering and Speers[18] showed that in the presence of sulfuric acid, only 30 min are required for complete conversion, compared to 8 days in the absence of acid.[19] Kinetic studies by Friess and Soloway also showed that the reaction was acid-catalyzed.[8] Since acid is generated as a byproduct during the reaction, autocatalysis may be observed, and the rate-determining step may change as acid is likely to affect the two steps differently.

In an effort to understand several of the key aspects of the Baeyer−Villiger reaction, including which step is rate-determining, what the effect of acid is on both steps, and what some of the controlling factors with respect to migratory aptitudes are, we embarked upon a combined theoretical and experimental study of the energetics of the Baeyer−Villiger oxidation of ketones. We were particularly interested in the effect of halogen substitutents on the relative activity and migratory aptitudes since two of us recently communicated a study in which surprising results were obtained in a series of fluorinated ketones.[7] Specifically, we showed that the spatial orientation of a fluorine substituent has a dramatic effect on the migratory aptitudes of the ketone substituents.

Thus, we examined the oxidation of acetone, 3-pentanone, fluoroacetone, chloroacetone, 2-fluoropentanone, and 2-chloropentanone via theoretical calculations using perfomic acid as the oxidant. A variety of fluorinated and chlorinated aliphatic ketones such as 3-fluoro and 3-chloroheptanone, among others, were studied experimentally using *m*CPBA[20] as the oxidant.[21,22]

Considering the importance of the Baeyer−Villiger reaction, it is surprising how few theoretical studies of this reaction have appeared. In 1997, Cardenas et al. reported ab initio studies on the oxidation of acetone with performic acid.[23] Only the second step of the reaction was examined. At the MP2/6-31G** level, the TS was found to lie 30 kcal/mol above the Criegee intermediate. In agreement with previous mechanistic studies,[24] it was found that cleavage of the oxygen−oxygen bond occurs concurrently with migration of the methyl group, whereas loss of the proton is delayed relative to that of the methyl group.

In a subsequent article, Cardenas et al.[25] used semiempirical methods (AM1 and PM3) to calculate the structure of the Criegee intermediate and the transition state for migration in the reaction of acetone with various peracetic and perbenzoic acids. Relative rate constants, as evaluated from the activation energies, correlated quite well with the experimentally determined Hammett electronic constants, supporting the notion that the second step of the reaction is rate-determining.

In the most comprehensive study to date, Okuno[26] examined the Baeyer−Villiger reaction of *p*-anisaldehyde and benzaldehyde with performic acid using the MP2/6-31G**//HF/3-21G method. The transition state for the formation of the Criegee intermediate, TS1, was also included in this study, as was the effect of acid catalyst.[27] It should be noted, however, that the Baeyer−Villiger reaction of benzaldehdyes generally proceeds by migration of *hydride* rather than the aryl group. Benzaldehyde itself, *p*-Cl, *p*-, and *m*-NO_2 benzaldehyde give exclusively hydride migration regardless of the pH, and *p*-anisaldehyde gives hydride migration at high pH and aryl migration at low pH.[12] In the case of aliphatic aldehydes, the ratio of hydride to alkyl

(2) Krow, G. R. *Org. React.* **1993**, *43*, 251.
(3) Renz, M.; Meunier, B. *Eur J. Org. Chem.* **1999**, 737.
(4) Criegee, R. *Justus Liebigs Ann. Chem.* **1948**, *560*, 128.
(5) Harmata, M.; Rashatasakhon, P. *Tetrahedron Lett.* **2002**, *43*, 3641.
(6) Harmata, M.; Rashatasakhon, P. *Org. Lett.* **2000**, *2*, 2913.
(7) Crudden, C. M.; Chen, A. C.; Calhoun, L. A. *Angew. Chem., Int. Ed.* **2000**, *39*, 2851.
(8) Friess, S. L.; Soloway, A. H. *J. Am. Chem. Soc.* **1951**, *73*, 3968.
(9) Hawthorne, M. F.; Emmons, W. D. *J. Am. Chem. Soc.* **1958**, *80*, 6398.
(10) Mitsuhashi, T. M.; Miyadera, H.; Simamura, O. *J. Chem. Soc., Chem. Commun.* **1970**, 1301.
(11) Palmer, B. W.; Fry, A. *J. Am. Chem. Soc.* **1970**, *92*, 2580.
(12) Reyes, L.; Castro, M.; Cruz, J.; Rubio, M. *J. Phys. Chem. A* **2005**, *109*, 3383.
(13) (a) Ogata, Y.; Sawaki, Y. *J. Org. Chem.* **1969**, *34*, 3985. (b) Ogata, Y.; Sawaki, Y. *J. Org. Chem.* **1972**, *37*, 2953.
(14) Ogata, Y.; Sawaki, Y. *J. Am. Chem. Soc.* **1972**, *94*, 4189.
(15) Singleton, D. A.; Szymanski, M. J. *J. Am. Chem. Soc.* **1999**, *121*, 9455.
(16) Friess, S. L. *J. Am. Chem. Soc.* **1949**, *71*, 14215.
(17) Friess, S. L.; Farnham, N. *J. Am. Chem. Soc.* **1950**, *72*, 5518.
(18) Doering, W. v. E.; Speers, L. *J. Am. Chem. Soc.* **1950**, *72*, 5515.
(19) The extent of catalysis was substrate-dependent, and the results were complicated by instability of the products in the presence of acid.
(20) *m*CPBA = *m*-chloroperbenzoic acid.
(21) Kitazume, T.; Kataoka, J. *J. Fluorine Chem.* **1996**, *80*, 157.
(22) Itoh, Y.; Yamanaka, M.; Mikami, K. *Org. Lett.* **2003**, *5*, 4803.
(23) Cardenas, R.; Cetina, R.; Lagunez-Otero, J.; Reyes, L. *J. Phys. Chem. A* **1997**, *101*, 192.
(24) Doering, W. v. E.; Speers, L. *J. Am. Chem. Soc.* **1950**, *72*, 5515.
(25) Cardenas, R.; Reyes, L.; Lagunez-Otero, J.; Cetina, R. *J. Mol. Struct. Theochem* **2000**, *497*, 211.
(26) Okuno, Y. *Chem.−Eur. J.* **1997**, *3*, 212.
(27) All of these values are ΔH_{liq} values.
(28) Anoune, N.; Hannachi, H.; Lanteri, P.; Longeray, R.; Arnaud, C. *J. Chem. Educ.* **1998**, *75*, 1290.

SCHEME 1. Uncatalyzed Baeyer−Villiger Reaction of Ketones 1a−f with Performic Acid

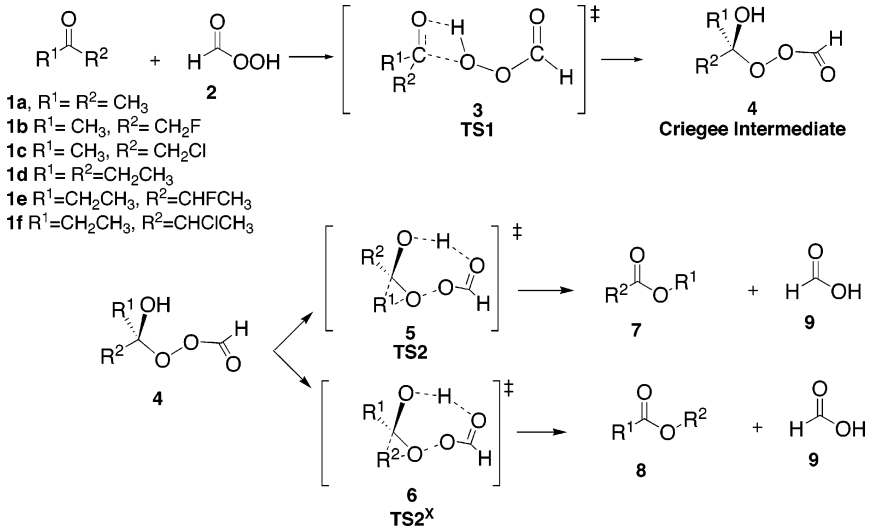

migration was found to depend critically on the solvent.[30] These facts unfortunately complicate correlation of the theoretical results with experimental observations since only aryl migration was modeled in the Okuno study. Theoretical studies of the oxidation of aldehydes with peroxycarboxylic acids,[28] of acetone with hydrogen peroxide as oxidant,[29] and of the effect of solvent on the oxidation of aldehydes[30] have also appeared.

Our study constitutes the first example of a full theoretical treatment of both steps of the Baeyer−Villiger oxidation of a ketone with a peracid, which is the method most commonly employed in synthesis. In addition, we report experimental studies on the Baeyer−Villiger oxidation of several representative fluoro and chloroketones, providing significant experimental support for the conclusions drawn in the theoretical study.

2. Theoretical Studies

Computational Methods. Geometry optimizations were performed with the Gaussian 98 programs,[31] using Hartree−Fock (HF), second-order Moeller−Plesset perturbation (MP2), and density functional theory (DFT) methods with the B3LYP[32] hybrid functional, at various levels of basis set. Results will be reported for the 6-31++G** basis set having diffuse functions and polarization functions both on the hydrogens and the first-row atoms.

In the following sections, energy differences ΔE, enthalpy differences ΔH, and Gibbs free energy differences ΔG, all relative to the reactants, will be presented. The ΔE's are differences in the calculated total (electronic) energies, without adjustment for zero-point energies (ZPE) or thermal effects. The enthalpy changes, ΔH, and Gibbs free-energy changes, ΔG, were calculated for standard temperature and pressure. ZPE corrections are included in ΔH and ΔG, but not in ΔE.

Results will also be given for energies and Gibbs free energies of solvation. For this purpose, dichloromethane ($\epsilon = 8.93$) has been chosen as solvent. The polarizable continuum model (PCM) method,[33,34] as implemented in Gaussian 98, has been applied to the gas-phase-optimized geometries, with the same DFT functional and basis set (B3LYP/6-31++G**) employed before.

General Reaction Profile. The reaction of acetone (**1a**) with performic acid (**2**) produces methyl acetate (**7a**) and formic acid (**9**) via the Criegee intermediate (**4**) (Scheme 1). Similarly, oxidation of 3-pentanone (**1d**) produces ethylpropionate (**7d**). For the halogenated substrates (**1b**, **c**, **e**, and **f**), migration of each substituent gives rise to a different product via different transition states. Inclusion of formic acid in the reaction scheme has a significant effect on the geometry of the transition states and energetics of the reaction (Scheme 2).[35]

As shown in Scheme 2, formic acid acts as a hydrogen bond donor and acceptor during the addition of performic acid to the ketone. This changes the geometry of the addition from a strained four-membered ring to a more favorable six-membered ring. The involvement of formic acid in the second step is similar, but in this case, the ring size changes from a seven-membered ring (uncatalyzed) to a nine-membered ring (catalyzed).

Results for Acetone, Fluoroacetone, and Chloroacetone. In Table 1, the energy, enthalpy, and free energy differences, relative to the reactants, of the Criegee intermediates, the two transition states, and the products are given for acetone, fluoroacetone, and chloroacetone in the presence and absence of acid.

For the substrates examined, ΔE and ΔH differ by no more than 2 kcal/mol. However, significant differences exist between ΔE and ΔG. For the Criegee intermediate, ΔG is generally about 15 kcal/mol higher than ΔE, and for the uncatalyzed transition states these values are 10−13 kcal/mol higher. Such systematic differences are mainly accounted for by differences in translational and rotational entropy. In the acid-catalyzed reactions, another 10−15 kcal/mol is added to ΔE because of the inclusion

(29) Carlqvist, P.; Eklund, R.; Brinck, T. *J. Org. Chem.* **2001**, *66*, 1193.
(30) Lehtinen, C.; Nevalainen, V.; Brunow, G. *Tetrahedron* **2001**, *57*, 4741.
(31) Frisch, M. J. et al. *Gaussian 98*, revision A.9; Gaussian, Inc.: Pittsburgh, PA, 1998.
(32) (a) Becke, A. D. *Phys. Rev.* **1988**, *A37*, 785. (b) Lee, C.; Yang, W.; Parr, R. G. *Phys. Rev.* **1988**, *B41*, 785. (c) Becke, A. D. *J. Chem. Phys.* **1993**, *98*, 5648. (d) Stevens, P. J.; Devlin, F. J.; Chablowski, C. F.; Frisch, M. J. *J. Phys. Chem.* **1994**, *80*, 11623.
(33) (a) Miertus, S.; Scrocco, E.; Tomasi, J. *Chem. Phys.* **1981**, *55*, 117. (b) Tomasi, J.; Miertus, S. *Chem. Phys.* **1982**, *65*, 239.
(34) Cossi, M.; Barone, V.; Cammi, R.; Tomasi, J. *Chem. Phys. Lett.* **1996**, *255*, 327.
(35) As described by Okuno, formic acid is assumed to catalyze the reaction without dissociation to H^+.

SCHEME 2. Effect of Acid Catalyst on the Baeyer−Villiger Oxidation of 1a−f

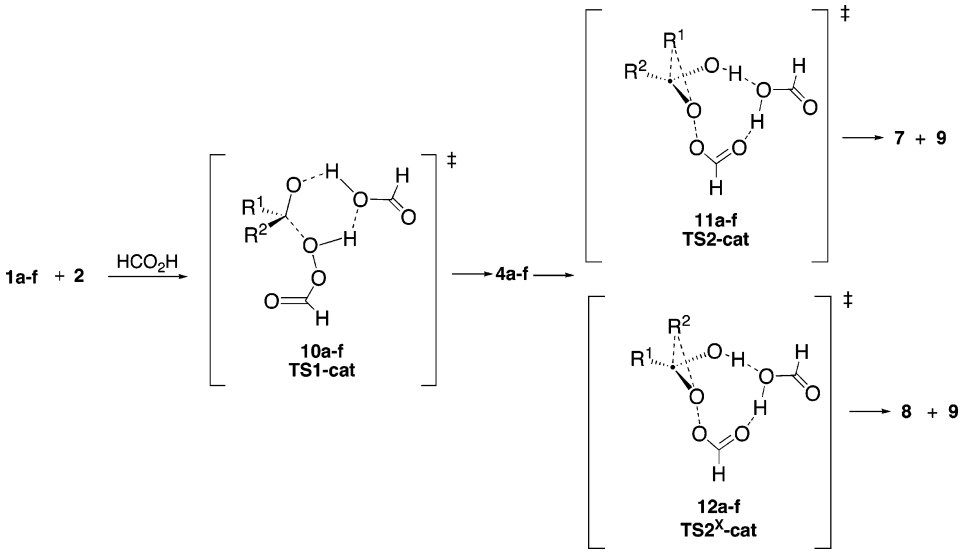

TABLE 1. Energies, Enthalpies, and Gibbs Free Energies for the Baeyer−Villiger Oxidation of Acetone, Fluoroacetone, and Chloroacetone[a]

	acetone (**1a**)			fluoroacetone (**1b**)			chloroacetone (**1c**)		
system	Δ*E*	Δ*H*	Δ*G*	Δ*E*	Δ*H*	Δ*G*	Δ*E*	Δ*H*	Δ*G*
TS1 (**3a−c**)	31.5	30.6	41.7	32.9	31.0	43.3	31.8	30.9	43.5
Criegee (**4a−c**)	−7.9	−5.2	7.5	−7.9	−5.8	7.8	−7.9	−5.8	8.3
TS2 (**5a−c**)	15.5	15.3	27.8	16.4	15.1	28.3	16.7	15.3	29.3
TS2[x] (**6b,c**)	−	−	−	15.3	14.5	28.0	16.3	15.4	29.3
TS1-cat (**10a−c**)	12.4	12.2	40.7	15.4	14.3	38.1	14.7	13.8	37.8
TS2-cat (**11a−c**)	9.5	10.6	38.6	12.1	12.2	35.0	11.7	11.9	35.4
TS2[x]-cat (**12b,c**)	−	−	−	9.3	9.9	32.8	9.9	10.4	33.8
prod (**7a−c**)	−68.7	−66.4	−67.7	−65.7	−64.0	−63.9	−66.3	−64.5	−64.3
prod[x] (**8b,c**)	−68.7	−66.4	−67.7	−75.0	−73.3	−73.1	−71.7	−70.2	−69.8

[a] All values are given in kcal/mol relative to reactants, using performic acid as the oxidant and formic acid as the catalyst. Only results for B3LYP/6-31++G** are provided. TS2[x]-cat refers to the acid-catalyzed second transition state in which the halogenated carbon is migrating, and all other transition states and products are numbered accordingly.

of a molecule of acid in the transition state, leading to an increase of about 28 kcal/mol in Δ*G* for acetone, and about 23−24 kcal/mol for the other systems.

Interestingly, the calculations predict that the first step will be rate-determining for all ketones examined. Activation energies of more than 30 kcal/mol are obtained for TS1 in the absence of acid. Presumably, the poor trajectory enforced by the necessity of transferring the peracid proton (Scheme 1) and forming the C−O bond at the same time is responsible for the high energy of the uncatalyzed TS. Activation energies (Δ*E*) for the second TS are much lower, ranging from about 10 to 16 kcal/mol.

The addition of acid dramatically decreases the Δ*E* of the first transition state, presumably because of the more favorable angle of attack. In the case of acetone, the Δ*E* of the first transition state drops from 31.5 to 12.4 kcal/mol. Significant decreases in energy, on the order of 16 kcal/mol, are also obtained upon inclusion of acid in TS1 for the reaction of **1b** and **1c**. Formic acid has less of an effect on the energies of the second transition states, however, only decreasing them by 4−6 kcal/mol.

However, as expected, the enthalpic gain resulting from inclusion of acid in the transition structures is mostly lost once free energy is calculated. For acetone, Δ*G* (TS1-cat) is ca. 28.3 kcal/mol higher than Δ*E*. Similar effects are seen in the haloacetone series, although the difference between Δ*G* and Δ*E* is ca. 23 kcal/mol instead of 28. For the products, the Δ*G* values are very close to the Δ*E*'s and Δ*H*'s, since the number of molecules remains the same as one goes from reactants to products.

Results for 3-Pentanone, Fluoropentanone, and Chloropentanone. It is well-known that the methyl group has one of the lowest migratory aptitudes of simple aliphatic substituents and that the ease of migration (migratory aptitude) increases with increasing substitution. To examine these effects and move beyond the extreme case of acetone, we performed calculations on 3-pentanone and its halogenated derivatives (Table 2). For the Criegee intermediates, the values are very similar to those of the acetone systems given in Table 1. The uncatalyzed first transition states have Δ*E*'s in the 30 kcal/mol range and Δ*G*'s in the 40 kcal/mol range. Marked differences, however, are observed in the second transition states. For TS2-cat, Δ*E* and Δ*H* are again about 5 kcal/mol lower than that for acetone, whereas Δ*G* is 10 kcal/mol lower.

Interestingly, the catalyzed first transition state is also decreased by almost 8 kcal/mol (free energy) for 3-pentanone compared to acetone, indicating that *the larger alkyl substituent decreases the TS for addition as well as migration*. Although the effect of additional substituents on the Baeyer−Villiger reaction has routinely been interpreted in terms of facilitating the migration, it is interesting to note that there is a substantial effect on the first transition state, which remains rate-determining. As in the case of acetone, once the Δ*G* of the reaction is

TABLE 2. Energies, Enthalpies, and Gibbs Free Energies for the Baeyer−Villiger Reaction of 3-Pentanone, 2-Fluoro-3-pentanone, and 2-Chloro-3-pentanone[a]

	pentanone			fluoropentanone			chloropentanone		
system	ΔE	ΔH	ΔG	ΔE	ΔH	ΔG	ΔE	ΔH	ΔG
TS1 (**3d**−**f**)	30.6	28.8	41.3	33.9	32.9	45.0	31.8	31.2	43.3
Criegee (**4d**−**f**)	−7.6	−5.8	8.3	−6.3	−4.4	9.2	−5.3	−3.4	10.4
TS2 (**5d**−**f**)	10.9	10.0	23.9	12.4	11.4	25.2	13.5	12.7	26.6
TS2^x (**6e**,**f**)	−	−	−	12.2	11.6	25.3	16.3	15.8	29.2
cat-TS1 (**10d**−**f**)	10.9	10.0	33.1	14.7	13.6	37.7	15.7	14.8	38.3
cat-TS2 (**11d**−**f**)	4.4	5.0	28.5	6.1	6.3	29.3	7.4	7.4	31.5
cat-TS2^x (**12e**,**f**)	−	−	−	6.7	7.5	30.0	9.0	9.8	32.3
prod (**7d**−**f**)	−72.7	−71.4	−71.2	−69.9	−68.7	−68.7	−69.9	−68.4	−68.4
prod^x (**8e**,**f**)	−	−	−	−77.6	−76.4	−76.2	−73.5	−72.2	−72.4

[a] All values are given in kcal/mol relative to reactants, using performic acid as the oxidant and formic acid as the catalyst. Only results for B3LYP/6-31++G** are provided. cat-TS2^x refers to the acid-catalyzed second transition state in which the halogenated carbon is migrating, and all other transition states and products are numbered accordingly.

TABLE 3. Solvation-Adjusted Gibbs Free Energies (kcal/mol), with Dichloromethane as Solvent, for the Baeyer−Villiger Reaction of Acetone, Fluoroacetone, and Chloroacetone[a]

	acetone (**1a**)	fluoroacetone (**1b**)	chloroacetone (**1c**)
TS1	43.7 (2.0)	46.0 (2.7)	46.6 (3.1)
Criegee	10.4 (2.9)	10.6 (2.8)	11.3 (3.0)
TS2	29.5 (1.7)	30.6 (2.3)	31.7 (2.4)
TS2^x	−	30.4 (2.4)	31.4 (2.1)
TS1-cat	45.6 (4.9)	43.6 (5.5)	43.6 (6.3)
TS2-cat	43.4 (4.8)	40.2 (5.2)	40.8 (5.4)
TS2^x-cat	−	38.5 (5.7)	39.3 (5.5)
prod	−68.1 (−0.4)	−65.5 (−1.6)	−65.0 (−0.7)
prod^x	−	−74.0 (−0.9)	−70.5 (−0.7)

[a] Energies are relative to reactants, and results are given for calculations with B3LYP/6-31++G**, using the PCM method. ΔG of solvation is given in parentheses.

TABLE 4. Solvation-Adjusted Gibbs Free Energies (kcal/mol), in Dichloromethane as Solvent, for the Baeyer−Villiger Reaction of Pentanone, Fluoropentanone, and Chloropentanone[a]

	3-pentanone (**1d**)	fluoropentanone (**1e**)	chloropentanone (**1f**)
TS1	44.7 (3.4)	48.6 (3.6)	46.8 (3.5)
Criegee	12.6 (4.3)	12.9 (3.7)	14.5 (4.1)
TS2	26.7 (2.8)	27.9 (2.7)	29.5 (2.9)
TS2^x	−	28.2 (2.9)	31.9 (2.7)
TS1-cat	38.9 (5.8)	43.9 (6.2)	45.5 (7.2)
TS2-cat	35.1 (6.6)	35.9 (6.6)	38.4 (6.9)
TS2^x-cat	−	36.9 (6.9)	38.9 (6.6)
prod	−71.7 (−0.5)	−70.5 (−1.8)	−69.2 (−0.8)
prod^x	−	−77.1 (−0.9)	−73.0 (−0.6)

[a] Energies are relative to reactants, and results are given for calculations with B3LYP/6-31++G**, using the PCM method. ΔG of solvation is given in parentheses.

considered, the optimal reaction path for 3-pentanone is via acid catalysis for TS1, but not for TS2.

Fluorine and Chlorine Substitution. In the absence of acid, TS1 and TS2 of fluoroacetone are energetically similar to acetone. A very slight preference (less than 1 kcal) is noted for migration of CH_2F versus migration of CH_3 in **1b**. The ΔG's of both the first and second transition states are higher for chloroacetone than acetone by about 2 kcal/mol, while the catalyzed transition states are slightly lower for chloroacetone (by 3−5 kcal/mol). The uncatalyzed second transition states for migration of CH_3 and CH_2Cl are identical in energy. If the catalyzed second transition states for fluoroacetone and chloroacetone are examined, the migration of the halogenated carbon is preferred by 1.6−2.3 kcal/mol. Although significant at the transition state, these differences are not experimentally meaningful since the reaction presumably proceeds by the lower energy, uncatalyzed second transition state.

Interestingly, for the fluorine- and chlorine-substituted pentanones, TS1 and TS2 lie energetically well above those of unsubstituted pentanone itself. Migration of the two substituents is equi-energetic (ΔG) in the case of fluoropentanone (0.1 kcal/mol difference), while there is a significant advantage for migration of the nonhalogenated carbon in the case of chloropentanone (2.8 kcal/mol). Again, these numbers are for the ΔG's of the noncatalyzed second transition states.

Effect of Solvation. To assess the effect of solvation on the Criegee intermediate and on the activation energies, calculations were performed with dichloromethane ($\epsilon = 8.93$) as solvent, using the PCM method and B3LYP/6-31++G**. In Table 3, the calculated values of Gibbs free energy of solvation relative to the gas phase (ΔG_{solv}) are given in parentheses, along with the new values for the overall solvation-adjusted ΔG's relative to the reactants. Table 4 describes the pentanone series.

As shown in Table 3, the Criegee intermediate as well as both transition states have positive ΔG_{solv} values, implying that the reactants benefit more from solvation than the higher energy species, whereas the products, having negative values of ΔE_{solv} and ΔG_{solv}, are more stabilized than the reactants. For the Criegee intermediate and the noncatalyzed TSs, the increases are relatively small, between 1.7 and 3.0 kcal/mol for ΔG_{solv}. The trends remain the same, with little difference between the migratory aptitudes of the halogenated and nonhalogenated substituents and the lowest transition state energies corresponding to acetone, followed by fluoroacetone and chloroacetone.

In the acid-catalyzed systems, the ΔG_{solv} numbers typically increase by 5−6 kcal/mol. As seen earlier for the ΔG's of the reaction, the entropy of solvation of *one* cat-TS molecule is much lower than that of *three* molecules, from which these transition structures are built. Thus, the catalyzed second transition state is still ca. 10 kcal/mol higher than the uncatalyzed TS in all three substrates. The results are similar for the pentanone series, except slightly higher increases are observed.

The effect of including solvation in the calculations is to raise the free energy of all of the transition states, especially the ones that include acid catalysis. In terms of relative ordering of the various transition states, two main effects result. In the case of acetone, the uncatalyzed first transition state becomes *lower* in energy than the catalyzed version. For all other systems, the addition of acid still results in a lower transition state, despite the entropic penalties. The other effect of solvation is to slightly separate the energy of the transition states for migration of

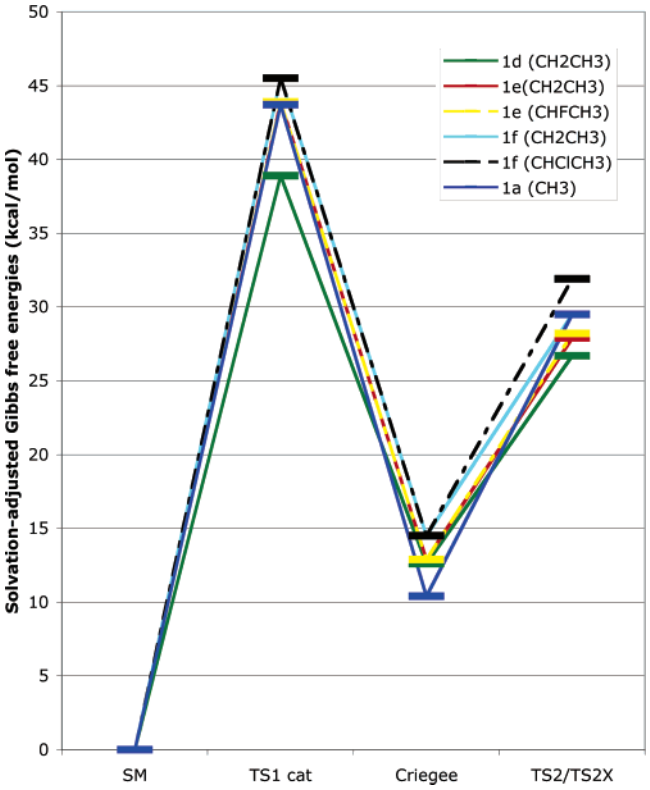

FIGURE 1. Relative free energies including solvation (dichloromethane) for the Baeyer−Villiger oxidation of **1a**, **d**, **e**, and **f**.

$CHFCH_3$ and CH_2CH_3 in fluoropentanone such that migration of the ethyl group is more favorable by 0.3 kcal/mol compared to migration of the fluorinated substituent (Figure 1). Overall, pentanone (green) is the most reactive substrate for both the first and the second transition states and chloroacetone (black) is the least.

Structures of Criegee Intermediates and Transition States. The calculated structures for the oxidation of acetone and pentanone are shown in Figure 2. In the halogenated series, three conformers were examined in each case, and in some cases, the difference between the different conformers was found to be dramatic. The most stable conformers are shown in Figure 2. A comparison of the halogen conformers is given in the Supporting Information.

Key bond distances for TS1, the Criegee intermediate, and TS1-cat are shown in Table 5. On the basis of the length of the incipient carbon−oxygen bond, the uncatalyzed first transition state is the most advanced for fluoro- and chloroacetone (**3b/c**, C^2-O^3 bond = 2.10 and 2.12 Å) and least for chloro- and fluoropentanone **3e/f** (C^2-O^3 = 2.23 Å). Interestingly, the length of the incipient O−H bond does not correlate with the C−O bond, being longest in **3b** (1.11Å) and shortest in **3e/f** (1.04 and 1.03 Å).

Despite the significant rearrangement required in TS1 for the inclusion of acid, the distance for the incipient C−O bond changes little for most of the compounds examined. A dramatic exception is fluoropentanone (**10e**), in which a 0.15 Å contraction is observed upon addition of acid. With this change, the most advanced transition states are observed for fluoroacetone and fluoropentanone, with C^2-O^3 bond lengths of 2.08 Å in both cases.

The bond distances in the Criegee intermediates are remarkably constant across the series, with the C−O bond length of the former carbonyl (C^2-O^1) at 1.39−1.40 Å, the O^3-O^4 bond at 1.44−1.45 Å, and the newly formed O^1-H^5 bond at 0.97 Å for all six ketones.

In all of the second transition states examined (Table 6), the O−O bond has stretched from 1.45 Å in the Criegee intermediates to 1.95−1.99 Å at the transition states. The incipient bond between the migrating CH_3 or CH_2CH_3 group (R^{mig} = migrating group) and the peroxide oxygen is remarkably constant, being 2.00−2.01 Å for the acetone series and 2.06−2.11 Å for the pentanone structures (uncatalyzed TS2). The transition state structures for migration of the halogenated substituents ($TS2^x$) all feature longer incipient XCH_2-O bonds than observed for the corresponding methyl migrations, implying that these transition states are less advanced. In the case of fluoroacetone, the difference is the smallest at 0.06 Å, but in all other examples, this bond is longer by about 0.1 Å. The O−O bond is also shorter in these cases, consistent with a less advanced transition state.

In the catalyzed second transition state there is little difference in the O−O bond for migration of CH_3 or CH_2X, with the exception of $TS2^x$-cat for chloropentanone (**12f**), where the O−O bond is relatively short at 1.92 Å. Elongation of $C-R^{mig}$ is observed in all cases for TS2 and $TS2^x$ upon addition of acid. The transfer of the hydroxyl proton from the Criegee intermediate to the acid catalyst (H^5-O^7) is significantly more advanced in the acetone series than the pentanone series.

3. Experimental Results

The relatively few published studies of oxidations of α-haloketones[36] indicate a preference for migration of the nonhalogenated carbon of varying magnitudes. However, these studies can be complicated by the fact that migration of the halogen-bearing carbon leads to a hydrolytically unstable species that can easily decompose under the reaction conditions (eq 2). Hydrolysis of the product from oxidation at the halogen-bearing carbon leads eventually to production of the corresponding aldehyde and HX, which then further increases the rate of hydrolysis of the ester, and the aldehyde itself is likely unstable under oxidizing conditions. This series of reactions complicates the analysis of the relative migratory aptitudes of these substrates, since low-yielding reactions with poor mass balances may actually indicate a propensity for migration of the halogenated substituent.

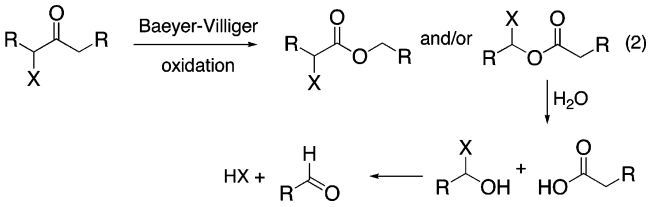

To assess the selectivity of the oxidation in halogenated systems, several fluoro- and chloroketones were prepared.

(36) (a) Itoh, Y.; Yamanaka, M.; Mikami, K. *Org. Lett.* **2003**, *5*, 4803. (b) Marigo, M.; Bachmann, S.; Halland, N.; Braunton, A.; Jorgensen, K. A. *Angew. Chem., Int. Ed.* **2004**, *43*, 5507. (c) Kobayashi, S.; Tanaka, H.; Amii, H.; Uneyama, K. *Tetrahedron* **2003**, *59*, 1547. (d) Shiozaki, M.; Arai, M. *J. Org. Chem.* **1989**, *54*, 3754. (e) Overberger, C. G.; Kaye, H. *J. Am. Chem. Soc.* **1967**, *89*, 5640. (f) Ahmad, M. S.; Farooq, Z. *Ind. J. Chem.* **1977**, 233. (g) Smissman, E. E.; Bergen, J. V. *J. Org. Chem.* **1962**, *27*, 2316. (h) Ali, S. M.; Roberts, S. M. *J. Chem. Soc., Perkin Trans. 1* **1976**, 1934. (i) Bollinger, J. E.; Courtney, J. L. *Aust. J. Chem.* **1964**, *17*, 440.

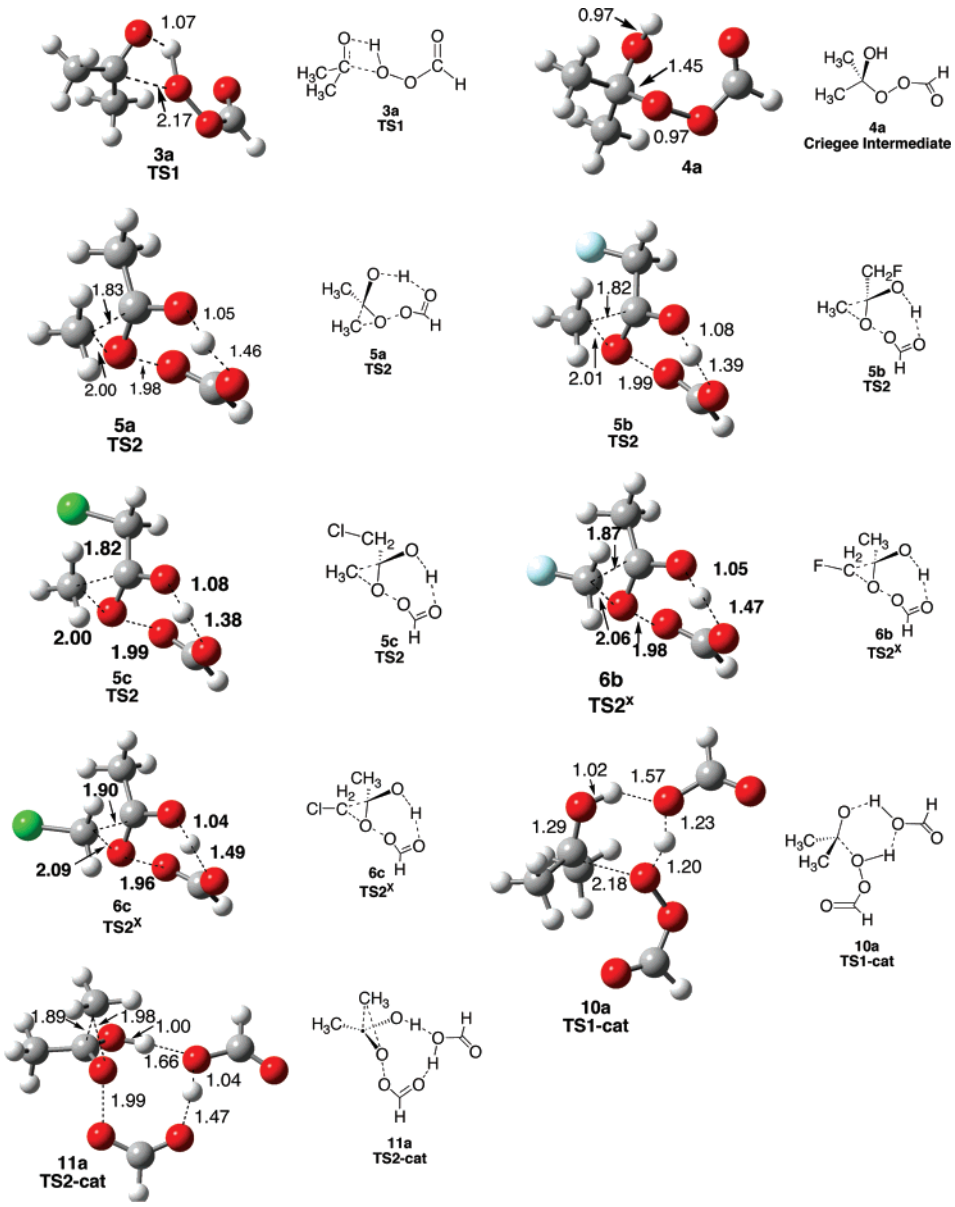

FIGURE 2. Calculated structures for key intermediates and transition states in the presence and absence of acid.

Unfortunately, fluoroacetone and chloroacetone were both highly resistant to oxidation, which is not surprising due to the very low migratory aptitude of the methyl substituent (or the CH_2X group). Rather than employ unusual catalysts or conditions to force this reaction to go to completion, we decided to employ representative ketones in our experimental study. Although it would be ideal to employ exactly the same ketones in both cases, we felt it was more desirable to have experimental conditions that were as close as possible to the simulated conditions. Considering the difficulties previously described with mass balance in the Baeyer−Villiger reactions of halogenated ketones, we were also concerned about the volatility of the pentanone derivatives. Thus, we prepared ketones **16**−**22**, which represent a relatively wide range of substrates, including straight-chain, cyclic, and benzylic aliphatic ketones. In particular, hexanone derivatives **19** and **22** are very close analogies of the pentanone derivatives examined in the theoretical studies. The synthetic routes employed for the preparation of the requisite ketones are shown in Scheme 3.

α-Haloketones **16**−**22** were then subjected to Baeyer−Villiger oxidation with *m*CPBA (Table 7). In all of the ketones examined, oxidation occurred preferentially at the nonhalogenated substituent. In the case of the α-fluoroketones, the selectivity was remarkably consistent throughout a range of substrates. In all cases, mass balances were between 83 and 93%. Both the 2-fluorocyclohexanone substrate **16** and the dibenzylketone **17** reacted with 70:30 preference for oxidation at the nonhalogenated carbon. Ketones **18** and **19**, which are better mimics of 2-fluoropentanone (**1e**), reacted with 75:25 and 67:33 selectivities, respectively. Again, the major isomer observed was that of oxidation at the nonhalogenated carbon. This ratio of products translates into a $\Delta\Delta G^{\ddagger}$ for their formation from the Criegee intermediate of 0.4−0.63 kcal/mol. This corresponds very well to the differences in free energy predicted for 2-fluoro-3-pentanone (**1e**) (0.3 kcal/mol, including entropy and using the solvation model, Table 4). In the case of **19**, which is the closest analogy to **1e**, we observe the best match with

TABLE 5. Key Bond Distances for TS1, Criegee, and TS1-cat

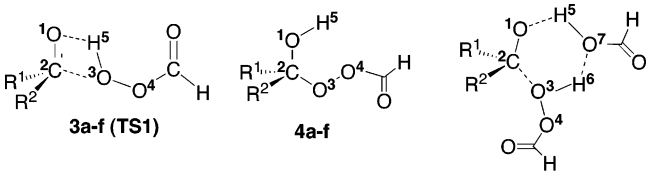

structure	C^2-O^1	C^2-O^3	O^1-H^5	O^3-H^5	O^7-H^6	O^7-H^5	O^3-H^6
TS1 (**3a**)	1.29	2.17	1.07	1.46	–	–	–
TS1 (**3b**)	1.30	2.10	1.11	1.39	–	–	–
TS1 (**3c**)	1.29	2.12	1. 05	1.52	–	–	–
TS1 (**3d**)	1.29	2.16	1.07	1	–	–	–
TS1 (**3e**)	1.29	2.23	1.04	1.60	–	–	–
TS1 (**3f**)	1.29	2.23	1.03	1.60	–	–	–
Criegee (**4a**)	1.40	1.45	0.97		–	–	–
Criegee (**4b**)	1.40	1.44	0.97		–	–	–
Criegee (**4c**)	1.40	1.44	0.97		–	–	–
Criegee (**4d**)	1.40	1.45	0.97		–	–	–
Criegee (**4e**)	1.39	1.45	0.97		–	–	–
Criegee (**4f**)	1.40	1.44	0.97		–	–	–
TS1-cat (**10a**)	1.29	2.18	1.02		1.23	1.57	1.20
TS1-cat (**10b**)	1.29	2.08	1.05		1.30	1.47	1.14
TS1-cat (**10c**)	1.29	2.15	1.04		1.26	1.49	1.17
TS1-cat (**10d**)	1.30	2.18	1.01		1.22	1.59	1.20
TS1-cat (**10e**)	1.29	2.08	1.04		1.29	1.50	1.15
TS1-cat (**10f**)	1.29	2.20	1.03		1.23	1.53	1.20

the theoretical studies ($\Delta\Delta G^{\ddagger}$ calculated = 0.3 kcal/mol and observed = 0.42 kcal/mol).

The oxidation of α-chloroketones **20**−**22** occurred significantly more slowly. For example, 3-chloroheptan-4-one (**22**) took 18 days to go to 22% conversion compared to the fluoro derivative **19**, which was 55% complete after just 4 days. This is in agreement with our calculations, which show that TS1, the rate-determining step, is highest in the chlorinated ketones. The calculations also predict a greater selectivity for the oxidation of the aliphatic substituent relative to the chlorinated substituent. For chloropentanone, $\Delta\Delta G^{\ddagger}$ is calculated to be on the order of 2.4 kcal/mol. For ketones **20** and **22**, we only observe the isomer resulting from oxidation at the nonhalogenated carbon. This is reasonable since a $\Delta\Delta G^{\ddagger}$ of 2.4 kcal/mol translates into a product ratio of ca. 97:3. In one case, chlorocyclohexanone **21**, we did observe the minor product in ca. 10% yield. This corresponds to a $\Delta\Delta G^{\ddagger}$ of 1.1 kcal/mol. Again, we note that the mass balances in all cases were high (usually greater than 80%) and therefore a high regioselectivity can be inferred.

4. Discussion

To the best of our knowledge, this study is the only theoretical examination of the *complete* Baeyer−Villiger reaction of a ketone, including both the addition and rearrangement steps. Six ketones were examined theoretically, and seven experimentally. Remarkable agreement was found between theory and experiment, even for ketones that had significant structural differences.

In the theoretical studies, the first step of the reaction was found to be rate-determining in the presence or absence of acid. The presence of acid has a significant effect on the enthalpy of the addition, improving the geometry of the attack and resulting in a decrease in ΔH of 16−19 kcal/mol. However, including an extra molecule in the transition state results in a large entropic penalty and a higher free energy. Thus, ΔH for TS1-cat is in the range of 10−15 kcal/mol, but ΔG is 33−40 kcal/mol (Tables 1 and 2). Despite this fact, addition to the ketone via the acid-catalyzed manifold is still more favorable for all ketones examined, with the exception of acetone (when solvation is included in the calculations). In this case, the addition via the uncatalyzed pathway is more favorable by 1.9 kcal/mol.

Inclusion of entropy in the calculations also has an effect on the Criegee intermediate. Examination solely of ΔE or ΔH leads to the untenable conclusion that this intermediate, which has never been isolated, is more stable than the starting material by 5−6 kcal/mol. However, when entropy is included in the calculations, the Criegee intermediate becomes 7−8 kcal/mol higher in energy than the starting materials.

For the second transition state, the inclusion of acid leads to a small decrease in ΔE and ΔH, but the entropic penalty is too great to counteract this. Thus, it is more energetically favorable for the reaction to proceed in the absence of acid catalyst for the second step.

The comparison between acetone and pentanone is also instructive. Experimentally, it has been shown that migration of methyl groups occurs extremely slowly, and therefore we chose to include the Baeyer−Villiger oxidation of 3-pentanone and its derivatives to permit more meaningful comparisons with experimental results. As expected, the reaction of pentanone was significantly enhanced relative to that of acetone. Relative to that of acetone, the calculated first and second transition states were **both** lowered by about 7 kcal/mol (solvated ΔG values). In fact, pentanone was the most reactive substrate of all those examined. The addition of a fluorine substituent on either acetone or pentanone had a slightly decelerating effect on both steps of the reaction. Surprisingly, the transition state for migration of the nonfluorinated carbon in fluoropentanone was only 0.3 kcal/mol lower than for migration of $CHFCH_3$. A larger preference of 2.6 kcal/mol was calculated for migration of CH_2-CH_3 versus $CHClCH_3$ in chloropentanone. The first transition state was elevated in all the chlorinated systems, implying that the overall rate will be slower, a fact borne out in experimental studies.

The few experimental studies in which halogenated ketones are subjected to Baeyer−Villiger oxidation are generally synthetic in focus, and thus the minor product (oxidation of the halogenated carbon) is rarely a consideration. Thus, to put our theoretical work in context, we carried out the Baeyer−Villiger oxidation of halogenated ketones, specifically to determine the regioselectivity of the reaction experimentally. In all of the fluoroketones examined, a ratio of approximately 70:30 in favor of migration of the nonfluorinated substituent was determined. This ratio translates to a $\Delta\Delta G^{\ddagger}$ of between 0.42 and 0.63 kcal/mol, which is remarkably similar to the predicted value of 0.3 kcal/mol for 2-fluoropentanone. Interestingly, the observed regioselectivity for oxidation of 3-fluorohexanone (0.42 kcal/mol) was actually closest to the calculated value of 0.3 kcal/mol.

In the chlorinated series, the preference for migration of the nonchlorinated substituent has been difficult to measure since in many cases only one product was observed. This is also consistent with the larger $\Delta\Delta G^{\ddagger}$ obtained in our calculations, which predict ratios on the order of 97:3 (nonhalogenated/halogenated). Our experiments with the chlorinated systems also revealed a significantly decreased rate of reaction, again consistent with theory, which showed that the transition state

TABLE 6. Key Bond Distances for TS2, TS2^x, TS2-cat, and TS2^x-cat

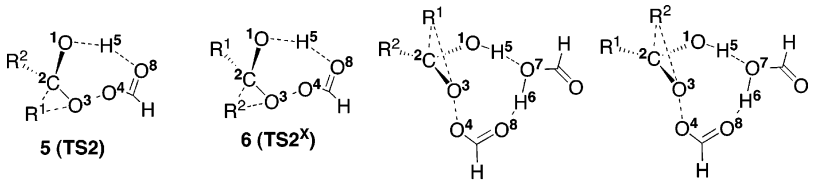

structure	C^2-R^{mig}	$R^{mig}-O^3$	O^3-O^4	O^1-H^5	H^5-O^8	H^5-O^7	O^7-H^6	H^6-O^8
TS2 (**5a**)	1.83	2.00	1.98	1.05	1.46	−		
TS2 (**5b**)	1.82	2.01	1.99	1.08	1.39	−		
TS2 (**5c**)	1.82	2.00	1.99	1.08	1.38	−		
TS2 (**5d**)	1.83	2.06	1.98	1.04	1.53	−		
TS2 (**5e**)	1.84	2.11	1.99	1.04	1.50	−		
TS2 (**5f**)	1.84	2.10	1.95	1.03	1.50	−		
TS2^x (**6a**)	1.83	2.00	1.98	1.05	1.46	−		
TS2^x (**6b**)	1.87	2.06	1.98	1.05	1.47	−		
TS2^x (**6c**)	1.90	2.09	1.96	1.04	1.49	−		
TS2^x (**6d**)	1.83	2.06	1.98	1.04	1.53	−		
TS2^x (**6e**)	1.88	2.17	1.94	1.02	1.56	−		
TS2^x (**6f**)	1.96	2.18	1.94	1.02	1.57	−		
TS2-cat (**11a**)	1.89	1.98	1.99	1.00	−	1.66	1.04	1.47
TS2-cat (**11b**)	1.90	1.98	2.01	1.01	−	1.60	1.06	1.43
TS2-cat (**11c**)	1.89	1.98	2.02	1.00	−	1.62	1.05	1.45
TS2-cat (**11d**)	1.88	2.09	1.96	0.99	−	1.73	1.03	1.52
TS2-cat (**11e**)	1.90	2.10	1.99	0.99	−	1.70	1.03	1.51
TS2-cat (**11f**)	1.89	2.09	1.96	.99	−	1.70	1.03	1.52
TS2^x-cat (**12a**)	1.88	1.98	1.99	1.00	−	1.66	1.04	1.47
TS2^x-cat (**12b**)	1.93	2.04	1.98	0.99	−	1.67	1.04	1.48
TS2^x-cat (**12c**)	1.97	2.10	1.97	0.99		1.68	1.03	1.50
TS2^x-cat (**12d**)	1.88	2.09	1.96	0.99	−	1.73	1.03	1.52
TS2^x-cat (**12e**)	1.97	2.19	1.94	0.98	−	1.76	1.02	1.55
TS2^x-cat (**12f**)	2.00	2.19	1.92	0.98		1.77	1.02	1.56

SCHEME 3. Preparation of Ketones 16−22

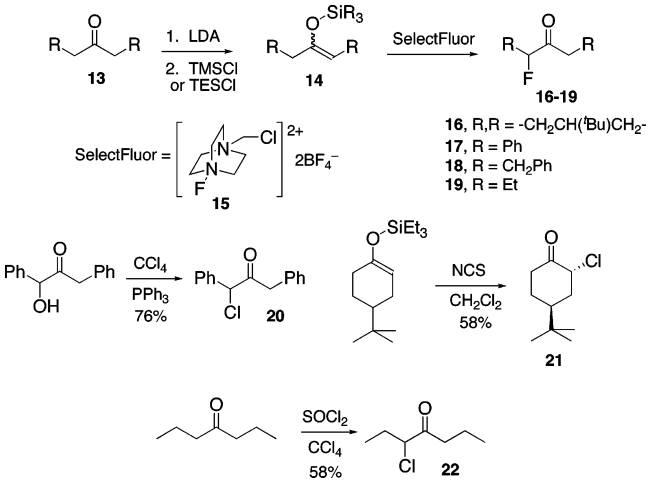

for attack at the carbonyl was highest in the case of the chlorinated substituents.

5. Summary and Conclusions

Several interesting features of the Baeyer−Villiger reaction have been revealed in our combined theoretical and experimental study. The reaction of acetone and 3-pentanone with performic acid is highly exothermic, with the products lying on average 60−80 kcal/mol lower in energy than the starting materials. The first step is rate-determining for all substrates examined, even in the presence of acid. The inclusion of entropy in the calculations is vital since it makes a significant difference in the predicted energy of the Criegee intermediates and both transition states. Acid catalysts generally decrease the ΔG of the first transition state, but increase the ΔG of the second one. Solvation stabilizes the products more than the starting materials and the starting materials more than the transition states or Criegee intermediate. The optimal reaction path for acetone proceeds over the uncatalyzed step for both TS1 and TS2, whereas the reaction with pentanone proceeds best via TS1-cat and TS2.

Relative to that of the other ketones examined in this study, migration of the ethyl group in pentanone seems to be the most energetically favorable. The introduction of a fluorine substituent decreases the migratory aptitude by a surprisingly moderate amount, both experimentally and theoretically. Chlorination decreases the experimentally observed rate of reaction, consistent with theoretical predictions. Both theory and experiment show the relative propensity for migration of a chlorinated substituent to be significantly attenuated relative to a nonhalogenated substituent. Work is ongoing to extend both the theoretical and experimental work to other classes of substrates including ethers, amines, and aromatic ketones.

6. Experimental Section

Commercial grade *m*CPBA was purified using an adaptation of the protocol described by Bortolini et al.[38] Diisopropylamine was distilled from CaH_2 and stored cold over potassium hydroxide pellets. *N*-Chlorosuccinimide was recrystallized from dichlo-

(37) Sever, R. R.; Root, T. W. *J. Phys. Chem. B* **2003**, *107*, 10848.
(38) Bortolini, O.; Campestrini, S.; Difuria, F.; Modena, G.; Valle, G. *J. Org. Chem.* **1987**, *52*, 5467.

TABLE 7. Baeyer−Villiger Oxidation of α-Haloketones

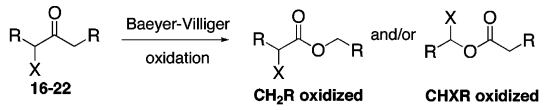

Entry	Substrate	Oxidation at CH_2R:CHXR[a]	Mass balance[b]	ΔΔG‡ (kcal/mol)
1	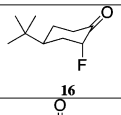 16	70 : 30	93%	0.49
2	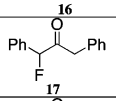 17	70 : 30	84%	0.49
3[c]	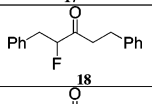 18	75 : 25	83%	0.63
4	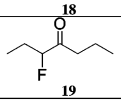 19	67 : 33	85%	0.42
5	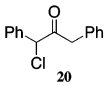 20	CH_2R-ox only product observed	88 %	–
6	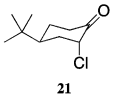 21	87 : 13	99%	1.1
7[d]	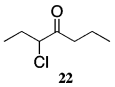 22	CH_2R-ox only product observed	76%	–

[a] Ratio of oxidation at the two substituents determined by ^{1}H NMR analysis of the crude reaction mixture. [b] Overall yield of the two products along with any recovered starting material. [c] Reaction only proceeded to 20% conversion. [d] Reaction only proceeded to 22% conversion.

romethane. The concentration of *n*-butyllithium used was determined via titration against BHT and fluorene or against *N*-benzylbenzamide. Commercially available 4-*tert*-butylcyclohexanone was recrystallized from hexanes. 4-Heptanone was distilled prior to use. All other chemicals were used without further purifications. Fluoroketone **16**,[39] the parent ketone of **18**,[40] and chloroketone **20**[41] were prepared according to literature procedures.

Synthesis of 2-Fluorodibenzylacetone (17). A 100-mL RBF was charged with a solution of diisopropylamine (0.62 mL, 4.7 mmol) in 20 mL of THF. This mixture was cooled to −78 °C and stirred at this temperature for 10 min. *n*-BuLi (2.2 mL of 2.16 M hexane solution, 4.8 mmol) was then added dropwise over 5 min, and the resulting pale yellow solution was stirred at −78 °C for a further 45 min. A solution of 1,3-diphenylacetone (0.98 g, 4.7 mmol) and chlorotriethylsilane (0.94 mL, 5.6 mmol) in 30 mL of THF was then added dropwise via a syringe. The reaction mixture was stirred cold for 1 h and then warmed to room temperature and stirred for a further 2 h. The reaction mixture was concentrated in vacuo, and the resulting residue was triturated with pentane (100 mL). The insoluable salts were filtered off to reveal, after concentration in vacuo, 1.23 g (83%) of the corresponding enol silyl ether. A portion of this material (1.14 g, 3.5 mmol) was then diluted with 30 mL of DMF. To this solution was added finely powdered Selectfluor (1.50 g, 4.23 mmol) as a suspension in 30 mL of DMF. The resulting mixture was stirred at 0 °C for 2 h and then at room temperature overnight. At 0 °C, the reaction was quenched with 40 mL of distilled water and extracted with diethyl ether (4 × 100 mL). The combined organic layers were washed with brine (200 mL), dried over Na_2SO_4, filtered, and concentrated in vacuo. The product mixture was purified by column chromatography (silica gel, 10:1 hexanes/ethyl acetate) to afford fluoroketone **17** as a white powder. Subsequent recrystallization from boiling hexanes gave 0.73 g (91%) of **17** as crystalline white plates. Spectra are consistent with those reported elsewhere.[42]

Synthesis of 2,9-Diphenyl-3-fluorononan-5-one (18). Following the procedure for the synthesis of **17**, diisopropylamine (0.54 mL, 4.1 mmol), *n*-BuLi (1.7 mL of 2.5 M hexane solution, 4.3 mmol), chlorotriethylsilane (0.94 mL, 5.6 mmol), and the parent ketone were reacted to give 0.76 g (71%) of the corresponding enol silyl ether. A portion of this material (0.70 g, 2.1 mmol) was then fluorinated with Selectfluor (1.34 g, 3.78 mmol). The crude product mixture thus obtained was then purified by column chromatography (silica gel, 30:1 hexanes/ethyl acetate) to give 0.67 g (73%) of **18**. ^{1}H NMR (400 MHz, $CDCl_3$) δ 7.3−7.6 (m, 10H), 4.73 (ddd, J = 49.0, 8.8, 4.0 Hz, 1H), 2.61−2.82 (m, 6H), 1.91−2.10 (m, 4H). ^{19}F NMR (376 MHz, $CDCl_3$) δ −196.0 (m).

Synthesis of 2-Fluoro-3-heptanone (19). LDA was generated by the dropwise addition of 1.37 M *n*-BuLi (25.5 mL, 35 mmol) to diisopropylamine (35.7 mmol, 5.0 mL) in 40 mL of dry THF. The LDA solution was cooled to −78 °C, and to this 4-heptanone (20.0 mmol, 2.8 mL) and trimethylsilyl chloride (39.4 mmol, 5.0 mL) were slowly added as a solution in 20 mL of dry THF. The reaction flask was left to warm to room temperature over 16 h. THF was removed in vacuo, and the reaction mixture was diluted with 20 mL of anhydrous DMF. Selectfluor (40.0 mmol, 14.2 g) was next added as a suspension in 20 mL of DMF at 0 °C and left to stir at ambient temperature for 16 h. The reaction was quenched with distilled water (100 mL) and extracted with diethyl ether (3 × 30 mL). Partial pressure distillation at 250 mmHg followed. Ketone **18** was isolated in the fraction boiling at 104−107 °C. Yield 44%. ^{1}H and ^{13}C NMR spectra are consistent with published data.[43]

Preparation of (±)-2-Chlorodibenzylacetone (20). In a 100-mL RBF equipped with a magnetic stir bar, 2-hydroxydibenzylacetone (0.091 g, 0.40 mmol) was suspended in 8 mL of CCl_4. This mixture was cooled to 0 °C, and then a solution of triphenylphosphine (0.13 g, 0.48 mmol) in 20 mL of CCl_4 was added. The reaction vessel was then fitted with an oven-dried reflux condenser, and the reaction suspension was refluxed in darkness for 10 h. After cooling to room temperature, 100 mL of pentane was added. The resulting suspension was then thoroughly triturated and filtered. The filtrate was concentrated to reveal a cloudy residue. The crude product mixture thus obtained was purified via column chromatography (silica gel, gradient elution, 30:1 to 20:1 to 15:1 hexane/ethyl acetate) to afford 93 mg (76% yield) of chloroketone **20**. Spectral data were consistent with literature data.[41] ^{1}H NMR (400 MHz, $CDCl_3$) δ 7.16−7.31 (m, 8H), 6.97 (m, 2H), 5.37 (s, 1H), 3.80 (d, J = 16.0 Hz, 1H), 3.64 (d, J = 16 Hz, 1H). ^{13}C {^{1}H} NMR (100 MHz, $CDCl_3$) δ 206.1, 136.3, 132.5, 129.5, 129.2, 128.8, 128.6, 127.1, 126.9, 78.1, 44.4.

Synthesis of *cis*-4-*tert*-Butylchlorocyclohexanone (21). A 250-mL RBF equipped with a magnetic stir bar and addition funnel was charged with a solution of enolsilyl ether **14**[44] (7.60 g, 33.6 mmol) in 50 mL of dried dichloromethane at 0 °C. A solution of freshly recrystallized *N*-chlorosucccinimide (5.40 g, 40.4 mmol) in 100 mL of dichloromethane was added dropwise via the addition funnel. The reaction mixture was stirred at 0 °C for 8 h and then was warmed to room temperature and allowed to stir for another 16 h. Upon recooling to 0 °C, the reaction was quenched with 100 mL of distilled water. The organic layer was separated and washed with brine (100 mL) and dried over Na_2SO_4, filtered, and concentrated in vacuo. The resulting oily mixture of products was isolated by repeated column chromatography (silica gel, 20:1

(39) Denmark, S. E.; Wu, Z. C.; Crudden, C. M.; Matsuhashi, H. *J. Org. Chem.* **1997**, *62*, 8288.
(40) Seebach, D.; Corey, E. J. *J. Org. Chem.* **1975**, *40*, 231.
(41) Fort, A. W. *J. Am. Chem. Soc.* **1962**, *84*, 2620.
(42) Rozen, S.; Menahem, Y. *J. Fluorine Chem.* **1980**, *16*, 19.

hexanes/ethyl acetate) to afford 3.74 g (59%) of ketone **21** along with about 8−10% of the trans isomer, which was separated by chromatography. The spectra obtained were identical to those reported elsewhere.[29]

Synthesis of 3-Chloro-4-heptanone (22). 4-Heptanone (5.03 mL, 36.00 mmol) was dissolved in 40 mL of anhydrous CCl_4 and maintained at 0 °C during the dropwise addition of sulfuryl chloride (2.90 mL, 36.10 mmol). The reaction flask was then warmed to 50 °C for 3.5 h. CCl_4 was removed by distillation at atmospheric pressure. Isolation of pure **22** was accomplished by column chromatography (silica gel, 8:1 hexanes/methylene chloride, R_f 0.41), 3.153 g (59% yield). **22** displayed spectra consistent with previously published data.[45]

Baeyer−Villiger Oxidation of *trans*-2-Fluoro-4-*t*-butylcyclohexanone (16).

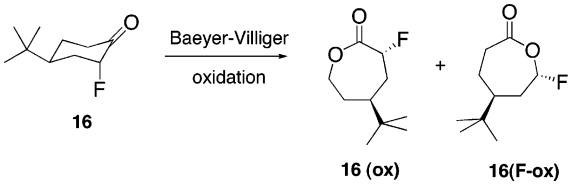

In a 25-mL RBF were combined fluoroketone **16** (446 mg, 2.59 mmol), *m*CPBA (530 mg, 3.07 mmol), and sodium bicarbonate (218 mg, 2.59 mmol) in 13 mL of HPLC grade chloroform. The resulting suspension was then stirred under a static nitrogen atmosphere in darkness at ambient temperature and monitored periodically via thin-layer chromatography. When the reaction was deemed complete, chloroform was removed in vacuo to reveal a white solid residue. The residue was then taken up in hexane (50 mL), and the resulting suspension was filtered. After washing the precipitate with copious amounts of hexane, we concentrated the filtrate in vacuo. The resulting yellow oil, after ^{1}H NMR analysis, was then purified via repeated column chromatography (silica gel, gradient elution, 14:1 to 12:1 hexane/ethyl acetate) to afford 291 mg (66% yield) of **16(ox)** and 120 mg (27% yield) of **16(F-ox)**.

Fluorolactone 16(ox): IR (NaCl) ν 1746 (s). ^{1}H NMR (400 MHz, $CDCl_3$) δ 5.39 (ddd, J = 49.2, 6.8, 3.2 Hz, 1H), 4.59 (ddd, J = 12.8, 8.8, 2.4 Hz, 1H), 4.25 (m, 1H), 2.36 (m, 1H), 2.11−2.18 (m, 1H), 1.60 (m, 3H), 0.91 (s, 9H). ^{13}C {^{1}H} NMR (100 MHz, $CDCl_3$) δ 170.1 (d, J = 22.0 Hz), 90.5 (d, J = 185.0 Hz), 67.7 (d, J = 6.0 Hz), 42.9 (d, J = 2 Hz), 32.6, 29.5 (d, J = 21.0 Hz), 29.4, 27.3. ^{19}F NMR (376 MHz, $CDCl_3$) δ −188.5 (m). MS (EI, 70 eV) *m*/*e*: 57 (C_4H_9, 100), 132 ($m^+ - C_4H_9$, 31), 173 ($m^+ - CH_3$, 6). HRMS (EI) *m*/*e*: calcd for $C_9H_{14}O_2F$ ($m^+ - CH_3$): 173.0979, found: 173.0970. TLC mobility, R_f 0.45 (in 4:1 hexane/ethyl acetate, visualized with PMA).

Fluorolactone 16(F-ox): IR (NaCl) ν 1756 (s). ^{1}H NMR (400 MHz, $CDCl_3$) δ 5.94 (dd, J = 50.0, 5.2 Hz, 1H), 2.80 (ddt, J = 14.2, 7.4, 2.0 Hz, 1H), 2.65 (td, J = 13.6, 2.0 Hz, 1H), 2.44 (ddt, J = 14.8, 5.2, 2.4 Hz, 1H), 2.03 (m, 1H), 1.76 (tt, J = 12.0, 2.4 Hz, 1H), 1.60 (m, 1H), 1.35 (m, 1H), 0.92 (s, 9H). ^{13}C {^{1}H} NMR (100 MHz, $CDCl_3$) δ 172.6, 106.6 (d, J = 231.0 Hz), 42.9 (d, J = 3.0 Hz), 35.3 (d, J = 4.0 Hz), 33.9 (d, J = 22.0 Hz), 32.7, 27.4, 23.6. ^{19}F NMR (376 MHz, $CDCl_3$) δ −131.7 (dd, J = 50.0, 32.0 Hz). MS (EI, 70 eV) *m*/*e*: 57 (C_4H_9, 100), 153 ($m^+ - CH_3 - HF$, 9), 173 ($m^+ - CH_3$, 1). HRMS (EI), *m*/*e*: calcd for $C_9H_{14}O_2F$ ($m^+ - CH_3$): 173.0979, found: 173.0969. TLC mobility, R_f 0.61 (in 4:1 hexane/ethyl acetate, visualized with *p*-anisaldehyde).

Baeyer−Villiger Oxidation of 2-Fluorodibenzylacetone (17). Following the optimized protocol outlined for the oxidation of fluoroketone **16**, fluoroketone **17** (112 mg, 0.49 mmol), *m*CPBA

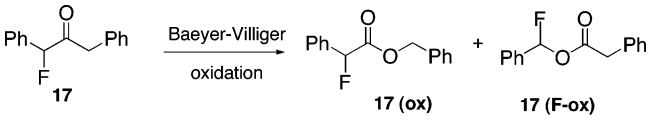

(102 mg, 0.59 mmol), and sodium bicarbonate (41 mg, 0.50 mmol) were reacted to give, after purification by column chromatography (silica gel, gradient elution, 14:1 to 12:1 to 10:1 hexane/ethyl acetate), 72 mg (60% yield) of **17(ox)** and 27 mg (24% yield) of **17(F-ox)**.

Fluorolactone 17(ox): IR (NaCl) ν 1760 (s). ^{1}H NMR (400 MHz, $CDCl_3$) δ 7.36 (m, 10H), 5.81 (d, J = 47.6 Hz, 1H), 5.20 (dd, J = 33.2, 12.0 Hz, 2H). ^{13}C {^{1}H} NMR (100 MHz, $CDCl_3$) δ 168.3, 134.9 (d, J = 18.3 Hz), 133.9, 129.6 (d, J = 2.4 Hz), 128.8, 128.6, 128.5, 128.1, 126.7, 89.3 (d, J = 184.9 Hz), 67.3. ^{19}F NMR (376 MHz, $CDCl_3$) δ −180.6 (d, J = 48.9 Hz). MS (EI, 70 eV), *m*/*e*: 91 (C_7H_7, 100), 244 (m^+, 17). HRMS (EI), *m*/*e*: calcd for $C_{15}H_{13}O_2F$ (m^+): 244.0900, found: 244.0908. TLC mobility, R_f 0.46 (in 8:1 hexane/ethyl acetate, visualized with UV and *p*-anisaldehyde).

Fluorolactone 17(F-ox): IR (NaCl) ν 1764 (s). ^{1}H NMR (400 MHz, $CDCl_3$) δ 7.36 (m, 10H), 7.21 (d, J = 55.2 Hz, 1H), 3.77 (d, J = 1.2 Hz, 2H). ^{13}C {^{1}H} NMR (100 MHz, $CDCl_3$) δ 169.6, 134.5 (d, J = 22.3 Hz), 132.7, 130.2 (d, J = 1.6 Hz), 129.3, 128.7, 128.6, 127.4, 126.1 (d, J = 5.5 Hz), 101.7 (d, J = 220.0 Hz), 41.0. ^{19}F NMR (376 MHz, $CDCl_3$) δ −123.0 (d, J = 54.9 Hz). MS (EI, 70 eV), *m*/*e*: 91 (C_7H_7, 83), 225 ($m^+ - F$, 23), 244 (m^+, 7). HRMS (EI), *m*/*e*: calcd for $C_{15}H_{13}O_2F$ (m^+): 244.0900, found: 244.0889. TLC mobility, R_f 0.54 (in 8:1 hexane/ethyl acetate, visualized with UV and *p*-anisaldehyde).

Baeyer−Villiger Oxidation of (±)-2,9-Diphenyl-3-fluornonan-5-one (18).

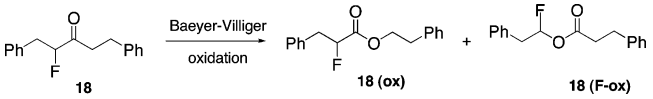

Following the optimized protocol outlined for the oxidation of fluoroketone **16**, fluoroketone **18** (665 mg, 2.34 mmol), *m*CPBA (466 mg, 2.7 mmol), and sodium bicarbonate (227 mg, 2.7 mmol) were reacted to give, after purification by way of column chromatography (silica gel, 30:1 hexane/ethyl acetate), 111 mg (16% yield) of **18(ox)** and 38 mg (6% yield) of **18(F-ox)**.

Fluorolactone 18(ox): ^{1}H NMR (400 MHz, $CDCl_3$) δ 7.14−7.31 (m, 10H), 4.86 (dt, J = 49.2, 6.0 Hz, 1H), 4.17 (t, J = 6.0 Hz, 2H), 2.79 (t, J = 6.8 Hz, 2H), 2.67 (t, J = 8.0 Hz, 2H), 2.13−2.24 (m, 2H), 1.98 (m, 2H). ^{19}F NMR (376 MHz, $CDCl_3$) δ −192.8 (m). TLC mobility, R_f 0.33 (in 20:1 hexane/ethyl acetate, visualized with UV and PMA).

Fluorolactone 18(F-ox): ^{1}H NMR (400 MHz, $CDCl_3$) δ 7.15−7.33 (m, 10H), 7.43 (dt, J = 56.2, 4.0 Hz, 1H), 3.38 (t, J = 8.0 Hz, 2H), 2.69 (t, J = 7.6 Hz, 2H), 2.52 (t, J = 7.6 Hz, 2H), 2.22 (m, 2H), 2.01 (m, 2H). ^{19}F NMR (376 MHz, $CDCl_3$) δ −129.2 (dt, J = 55.9, 18.0 Hz). TLC mobility, R_f 0.49 (in 20:1 hexane/ethyl acetate, visualized with UV and PMA).

Baeyer−Villiger Oxidation of 3-Fluoro-4-heptanone (19).

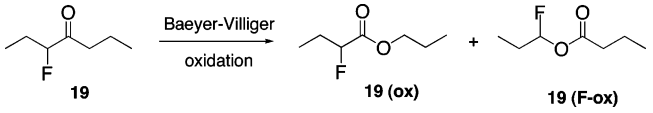

Following the optimized protocol outlined for the oxidation of fluoroketone **16**, fluoroketone **19** (857 mg, 6.48 mmol), *m*CPBA (1.350 g, 7.82 mmol), and sodium bicarbonate (546 mg, 6.50 mmol) were reacted to 55% conversion to afford a crude mixture containing **19(ox)** (64%) and **19(F-ox)** (36%).

(43) Enders, D.; Faure, S.; Potthoff, M.; Runsink, J. *Synthesis* **2001**, 2307.
(44) Denmark, S. E.; Dappen, M. S. *J. Org. Chem.* **1984**, *49*, 798.
(45) Marigo, M.; Bachmann, S.; Halland, N.; Braunton, A.; Jorgensen, K. A. *Angew. Chem., Int. Ed.* **2004**, *43*, 5507.

Fluorolactone 19 (F-ox): IR (neat) ν 1740 cm^{-1}. ^{1}H NMR (500 MHz, $CDCl_3$) δ 6.30 (dt, J = 55.9, 5.1 Hz, 1H), 2.38 (t, J = 7.4 Hz, 2H), 1.85 (m, 2H), 1.71 (m, 2H), 1.00 (m, 6H). ^{19}F NMR (400 MHz, $CDCl_3$) δ −146.34 (m). ^{13}C {^{1}H} NMR (500 MHz, $CDCl_3$) δ 172.30, 104.16 (d, J = 220.9 Hz), 36.34, 26.94 (d, J = 22.9 Hz), 22.30, 13.89, 7.55 (d, J = 5.9 Hz).

Fluorolactone 19(ox): IR (neat) ν 1762 cm^{-1}. ^{1}H NMR (500 MHz, $CDCl_3$) δ 4.88 (ddd, J = 49.1, 7.0, 4.5 Hz, 1H), 4.17 (t, J = 6.7 Hz, 2H), 1.95 (m, 2H), 1.70 (m, 2H), 1.00 (m, 6H). ^{19}F NMR (400 MHz, $CDCl_3$) δ −130.99 (m). ^{13}C {^{1}H} NMR (500 MHz, $CDCl_3$) δ 170.36, 90.28 (d, J = 184.2 Hz), 67.28, 26.22 (d, J = 1.5 Hz), 10.64, 9.19 (d, J = 4.2 Hz).

Baeyer−Villiger Oxidation of 2-Chlorobenzylacetone (20).

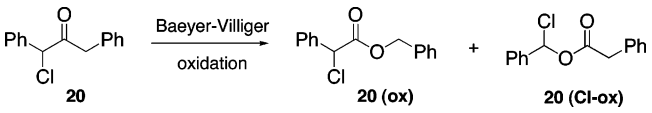

Following the optimized protocol outlined for the oxidation of fluoroketone **16**, chloroketone **20** (0.084 g, 0.34 mmol), *m*CPBA (0.070 mg, 0.41 mmol), and sodium bicarbonate (29 mg, 0.35 mmol) were reacted to give, after purification by way of column chromatography (silica gel, 40:1 hexane/ethyl acetate), 40 mg (45% yield) of **20(ox)**. A second fraction containing **20** (36 mg, 43% recovery) was also collected.

Chlorolactone 20(ox): IR (neat) ν 1752 cm^{-1}. ^{1}H NMR (400 MHz, $CDCl_3$) δ 7.02−7.29 (m, 10H), 5.46 (s, 1H), 5.23 (d, J = 12.4 Hz, 1H), 5.16 (d, J = 12.4 Hz, 1H). ^{13}C {^{1}H} NMR (100 MHz, $CDCl_3$) δ 173.0, 139.3, 131.4, 129.9, 128.8, 128.6, 127.4, 127.1, 126.9, 79.9, 71.7. HRMS (EI), *m*/*z*: calcd for $C_{15}H_{13}O_2Cl$ (m^+ − H): 260.0604, found: 260.0604.

Baeyer−Villiger Oxidation of *trans*-2-Chloro-4-*t*-butylcyclohexanone (21).

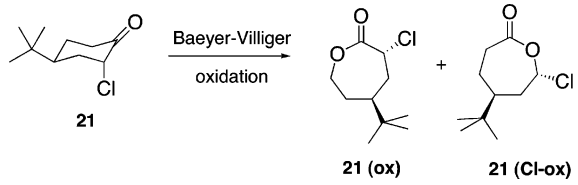

Following the optimized protocol outlined for the oxidation of fluoroketone **16**, chloroketone **21** (251 mg, 1.32 mmol), *m*CPBA (253 mg, 1.46 mmol), and sodium bicarbonate (121 mg, 1.44 mmol) were reacted to give, after purification by way of column chromatography (silica gel, gradient elution, 20:1 to 18:1 to 16:1 hexane/ethyl acetate), 23 mg (8% yield) of **21(Cl-ox)** and 154 mg (57% yield) of **21(ox)** as white solids.

Chlorolactone 21 (Cl-ox): ^{1}H NMR (400 MHz, $CDCl_3$) δ 6.29 (dd, J = 7.8, 3.2 Hz, 1H), 2.71 (ddd, J = 14.2, 7.0, 2.2 Hz, 1H), 2.41 (m, 2H), 2.03 (m, 2H), 1.40−1.52 (m, 2H), 0.93 (s, 9H). Note: compound too unstable and isolated in too small an amount to obtain ^{13}C NMR spectra. TLC mobility, R_f 0.29 (in 10:1 hexane/ethyl acetate, visualized with *p*-anisaldehyde).

Chlorolactone 21(ox): ^{1}H NMR (400 MHz, $CDCl_3$) δ 4.89 (dd, J = 6.4, 2.0 Hz, 1H), 4.78 (ddd, J = 12.8, 10.4, 1.2 Hz, 1H), 4.32 (ddd, J = 12.8, 6.2, 2.0 Hz, 1H), 2.24 (m, 1H), 2.13 (m, 1H), 1.87 (tt, J = 12.0, 2.8 Hz, 1H), 1.79 (m, 1H), 1.49 (dddd, J = 13.6, 12.0, 10.4, 2.0 Hz, 1H), 0.92 (s, 9H). ^{13}C {^{1}H} NMR (100 MHz, $CDCl_3$) δ 169.6, 68.6, 58.3, 43.9, 32.6, 31.4, 30.5, 27.5. TLC mobility, R_f 0.28 (in 10:1 hexane/ethyl acetate, visualized with *p*-anisaldehyde).

Baeyer−Villiger Oxidation of 3-Chloro-4-heptanone (22).

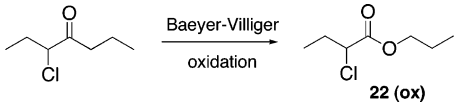

Following the optimized protocol outlined for the oxidation of fluoroketone **16**, chloroketone **22** (1.550 g, 10.43 mmol), *m*CPBA (1.985 g, 11.47 mmol), and sodium bicarbonate (876 mg, 10.43 mmol) were reacted for 18 days to afford a crude mixture containing **22** (78%) and **22(ox)** (22%). Bulb to bulb distillation (100 mmHg, 120 °C) afforded a sample (1.18 g, 76% mass balance) of **22** and **22(ox)**.

Chlorolactone 22(ox): IR (neat) ν 1747 cm^{-1}. ^{1}H NMR (500 MHz, $CDCl_3$) δ 4.25 (dd, J = 7.6, 6.0 Hz, 1H), 4.14−4.18 (m, 2H), 2.06−2.10 (m, 2H), 1.71−1.74 (m, 2H), 1.04−1.08 (m, 3H), 0.96−0.99 (m, 3H). ^{13}C {^{1}H} NMR (500 MHz, $CDCl_3$) δ 170.17, 67.85, 59.37, 28.81, 22.26, 11.04, 10.91. HRMS (CI), *m*/*z*: calcd for $C_7H_{13}O_2Cl$ (m^+ − H): 165.0682, found: 165.0724.

Supporting Information Available: Complete ref 31, spectra for selected compounds, discussion of effect of halogen conformers on the stability of TS2, and comparison with other theoretical work. This material is available free of charge via the Internet at http://pubs.acs.org.

JO0513966